Molecular Crystals and Liquid Crystals
Publication details, including instructions for authors and subscription information:
http://www.tandfonline.com/loi/gmcl16

Deformation of Nematic Liquid Crystals in Electric and Magnetic Fields as seen by Proton Nuclear Magnetic Resonance

A. Frieser [a] , H. Schmiedel [a] , B. Hillner [a] & A. Lösche [a]
[a] Sektion Physik der KMU, 7010, Leipzig, Linestr. 5, DDR
Version of record first published: 20 Apr 2011.

To cite this article: A. Frieser , H. Schmiedel , B. Hillner & A. Lösche (1984): Deformation of Nematic Liquid Crystals in Electric and Magnetic Fields as seen by Proton Nuclear Magnetic Resonance, Molecular Crystals and Liquid Crystals, 109:2-4, 245-262

To link to this article: http://dx.doi.org/10.1080/00268948408078710

Mol. Cryst. Liq. Cryst., 1984, Vol. 109, pp. 245–262
0026-8941/84/1094–0245/$18.50/0

Printed in the United States of America

Deformation of Nematic Liquid Crystals in Electric and Magnetic Fields as seen by Proton Nuclear Magnetic Resonance

A. FRIESER, H. SCHMIEDEL, B. HILLNER and A. LÖSCHE
Sektion Physik der KMU, 7010 Leipzig Linnestr. 5, DDR

(*Received November 23, 1983; in final form March 9, 1984*)

We have calculated the deformation of the director field within a nematic liquid-crystal cell when both external electric and magnetic fields are present. It can be proved experimentally that the line shape of proton nuclear magnetic resonance is strongly affected by the orientational distribution of the director.

The analysis of the NMR-line shape of LC-sandwich cells in this manner can yield various parameters relating to the liquid crystalline material.

1. INTRODUCTION

The orientation of the director in electrically nonconducting liquid crystal cells is determined by the elastic forces, the aligning action of the cell surfaces, and by external electric or magnetic fields.

By means of the elastic continuum theory, Saupe[1] was the first to calculate the orientational distribution of the nematic director caused by external magnetic fields in a LC cell. Later, Gruler *et al.*[2] and Deuling[3] studied the deformation of the homogeneous or homeotropic alignment of the director caused by a voltage applied to the cell. The results have been verified in different types of experiments such as measurements of capacitance or optical birefringence[2] in LC-sandwich samples.

In section 2 of this paper, we give an extension of the theory above, which allows us to calculate the orientational distribution of the

nematic director if both external fields, i.e., magnetic *and* electric, are present and make an arbitrary angle with each other.

In section 4 theoretical results are compared with experimental data obtained from proton nuclear magnetic resonance (NMR) spectra of LC sandwich samples. It is shown that in this case a deformation of the director field within the cell leads to a change of the NMR-line shape, thus providing an additional method for the determination of various LC parameters, e.g., the elastic constants.

2. THEORY

2.1. Deformation of nematic liquid crystals in electric and magnetic fields

We assume the nematic liquid crystal to be enclosed between two glass plates separated by a distance d. Let us first regard the case of homogeneous orientation depicted in Figure 1.

The orientation of the director at a distance z from the wall is described by the angle $\vartheta(z)$.

For the density of free energy of the nematic LC in Figure 1 we have the expression

$$F = F_{\text{elast.}} + F_{\text{magn.}} + F_{\text{electr.}} \tag{2.1}$$

$$F_{\text{elast.}} = \frac{1}{2}\left(\frac{d\vartheta}{dz}\right)^2\left(K_1\cos^2\vartheta + K_3\sin^2\vartheta\right) \tag{2.2}$$

$$F_{\text{magn.}} = -\frac{\mu_0}{2}\chi_a H^2\cos^2(\vartheta - \Phi) \tag{2.3}$$

$$F_{\text{electr.}} = \frac{1}{2}\frac{U^2}{d^2}\frac{\epsilon_\perp}{\tau(1 + \zeta\sin^2\vartheta)} \tag{2.4}$$

$F_{\text{elast.}}$ contains the elastic constants K_1 and K_3, and the magnetic energy $F_{\text{magn.}}$ depends on the angle $(\vartheta - \Phi)$ between the magnetic field $\mathbf{H}$ and the director $\mathbf{n}$. $\chi_a = \chi_\parallel - \chi_\perp$ is the anisotropy of the diamagnetic susceptibility and $\mu_0 = 4\pi \cdot 10^{-7}$ Vs/Am. The expression (2.4.) for the electric energy has been derived by Gruler[2] and Deuling[3]. U is the voltage applied to the cell and $\zeta = (\epsilon_\parallel - \epsilon_\perp)/\epsilon_\perp$, with the dielectric constants $\epsilon_\parallel$ parallel and $\epsilon_\perp$ perpendicular to the director. The integral

$$\tau = \frac{1}{d}\int_0^d \frac{dz}{1 + \zeta\sin^2\vartheta} = \frac{C_\perp}{C} \tag{2.5}$$

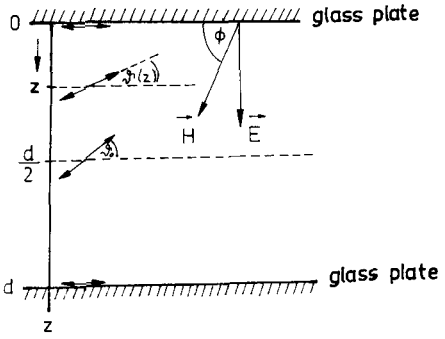

FIGURE 1 Cell geometry in the case of homogeneous orientation of the nematic director (strong anchoring). Electric field **E**, magnetic field **H**; the normal to the glass plates and the nematic director are assumed to be in one plane.

is the ratio between the capacitance $C_\perp$ of the undeformed LC-cell (director perpendicular to the normal to the plates) and the capacitance C in the case of deformation ($\vartheta_0 \neq 0$). To obtain the deformation $\vartheta(z)$ of the nematic liquid crystal in the case where one has simultaneously strong electric and magnetic fields, we integrated the Euler-Lagrange equation

$$\frac{\partial F}{\partial \vartheta} - \frac{d}{dz}\left(\frac{\partial F}{\partial \vartheta'}\right) = 0 \tag{2.6}$$

with F containing all three terms of Eq. (2.1.). Using the boundary conditions indicated in Figure 1 we get

$$\frac{2z}{d} = \frac{2}{\pi}\int_0^{\vartheta(z)} d\vartheta \left\{ \frac{1 + \eta \sin^2\vartheta}{(\sin^2\vartheta_0 - \sin^2\vartheta)R} \right\}^{1/2} \tag{2.7}$$

with $\eta = (K_3 - K_1)/K_1$ and

$$R = \left(\frac{U}{U_c}\right)^2 \frac{1}{\tau^2(1 + \zeta \sin^2\vartheta_0)(1 + \zeta \sin^2\vartheta)} + \left(\frac{H}{H_c}\right)^2 \left(-\cos 2\Phi + \frac{\sin 2\Phi}{\tan(\vartheta_0 + \vartheta)}\right). \tag{2.8}$$

$$U_c = \pi\left[K_1/(\epsilon_\parallel - \epsilon_\perp)\right]^{1/2} \tag{2.9}$$

and

$$H_c = (\pi/d)[K_1/\mu_0\chi_a]^{1/2} \tag{2.10}$$

are natural units of voltage and magnetic field.

To perform the integration in Eq. (2.7), one has to fix the maximum angle of deformation ϑ_0 and the value of τ in such a manner as to obey simultaneously the equations

$$\frac{2}{\pi}\int_0^{\vartheta_0} d\vartheta \left\{ \frac{1 + \eta \sin^2\vartheta}{(\sin^2\vartheta_0 - \sin^2\vartheta) R} \right\}^{1/2} = 1 \qquad (2.11)$$

and

$$\frac{2}{\pi}\int_0^{\vartheta_0} d\vartheta \frac{1}{1 + \vartheta \sin^2\vartheta} \left\{ \frac{1 + \eta \sin^2\vartheta}{(\sin^2\vartheta_0 - \sin^2\vartheta) R} \right\}^{1/2} = \tau. \qquad (2.12)$$

Eqs. (2.7), (2.11) and (2.12) can be simplified to the pure magnetic case[1] or the pure electric case[2,3] putting $U = 0$ or $H = 0$ in Eq. (2.8). If only the magnetic field H is present, Eq. (2.11) is sufficient to determine H/H_c as a function of ϑ_0[1], and in the pure electric case ($H = 0$), from Eq. (2.12) alone we can calculate ϑ_0 for given values of U/U_c.[3] In our case both U and H are different from zero and the determination of ϑ_0 as a function of U/U_c and H/H_c is more complicated.

Assuming $U \neq 0$ we define a parameter $\mathscr{H}$ as

$$\mathscr{H} = \frac{H}{H_c} \cdot \frac{U_c}{U} \cdot \tau \cdot (1 + \zeta \sin^2\vartheta_0)^{1/2} \qquad (2.13)$$

Eqs. (2.11) and (2.12) then can be rewritten

$$(1 + \zeta \sin^2\vartheta_0)^{1/2} \cdot \frac{2}{\pi}\int_0^{\pi/2} d\varphi \left\{ \frac{1 + \eta \sin^2\vartheta_0 \sin^2\varphi}{(1 - \sin^2\vartheta_0 \sin^2\varphi) \tilde{R}} \right\}^{1/2} = \frac{U}{U_c} \cdot \frac{1}{\tau} \qquad (2.14)$$

$$(1 + \zeta \sin^2\vartheta_0)^{1/2} \cdot \frac{2}{\pi}\int_0^{\pi/2} d\varphi \frac{1}{1 + \zeta \sin^2\vartheta_0 \sin^2\varphi} \left\{ \frac{1 + \eta \sin^2\vartheta_0 \sin^2\varphi}{(1 - \sin^2\vartheta_0 \sin^2\varphi) \tilde{R}} \right\}^{1/2} = \frac{U}{U_c} \qquad (2.15)$$

with

$$\tilde{R} = \frac{1}{1 + \zeta \sin^2\vartheta_0 \sin^2\varphi} + \mathscr{H}^2\left(-\cos 2\Phi + \frac{\sin 2\Phi}{\tan[\vartheta_0 + \arcsin(\sin\vartheta_0 \sin\varphi)]} \right) \quad (2.16)$$

Now, with fixed values of ϑ_0 and $\mathscr{H}$, Eqs. (2.14) and (2.15) give U/U_c and τ. Then from Eq. (2.13) H/H_c can be obtained. In Figures 2, 3 and 4, some results for the numerical evaluation of ϑ_0 as function of parameters U/U_c, H/H_c, Φ, η and ζ are shown.

Figure 2 shows the angle ϑ_0 *versus* U/U_c with $\Phi = 0°$ and $\zeta = 1$, $\eta = 0.5$ for different values of H/H_c. It is clear that the threshold voltage, with higher ratios H/H_c, is shifted to higher values.

From Figure 3 the changes of ϑ_0 with variation of the LC-parameters η and ζ can be seen. H/H_c was fixed to be $H/H_c = 3.82$ and $\Phi = 2°$.

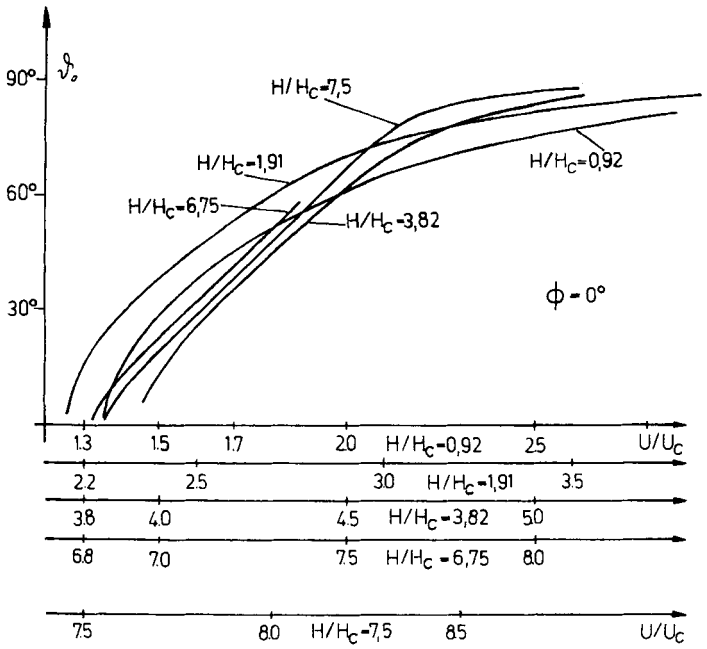

FIGURE 2 ϑ_0 *versus* U/U_c for various values of H/H_c. Calculations have been performed for $\Phi = 0°$, $\zeta = 1$ and $\eta = 0.5$.

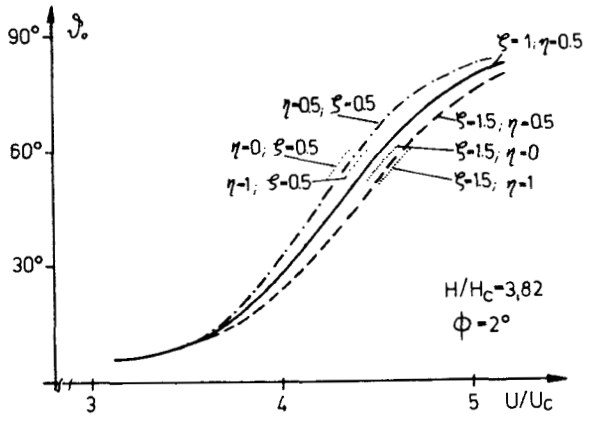

FIGURE 3 Calculated values of ϑ_0 *versus* U/U_c for different parameters η and ζ.

In Figure 4, ϑ_0 is plotted *versus* U/U_c for different directions Φ of the magnetic field with strength $H/H_c = 3.82$ and $\zeta = 1$, $\eta = 0.5$. The orientation $\vartheta(z)$ of the director for $H/H_c = 3.82$ with $\Phi = 2°$ and $\Phi = 35.3°$ can be seen in Figure 5. At the glass plate ($z = 0$) we have always $\vartheta(0) = 0$, followed by a monotonous growth of $\vartheta(z)$ to $\vartheta(d/2) = \vartheta_0$ in the middle of the cell. The formula and graphics given above apply also to the case of homeotropic orientation by replacing the angles $\vartheta \to \pi/2 - \vartheta$, $\Phi \to \pi/2 - \Phi$, which is equivalent to the substitution of $\epsilon_{\parallel} \leftrightarrow \epsilon_{\perp}$ and $K_3 \leftrightarrow K_1$ as was pointed out by Deuling[3] in the pure electric case.

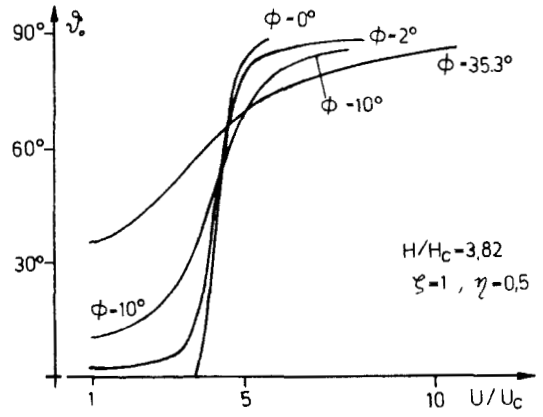

FIGURE 4 ϑ_0 *versus* U/U_c for some different directions Φ of the magnetic field.

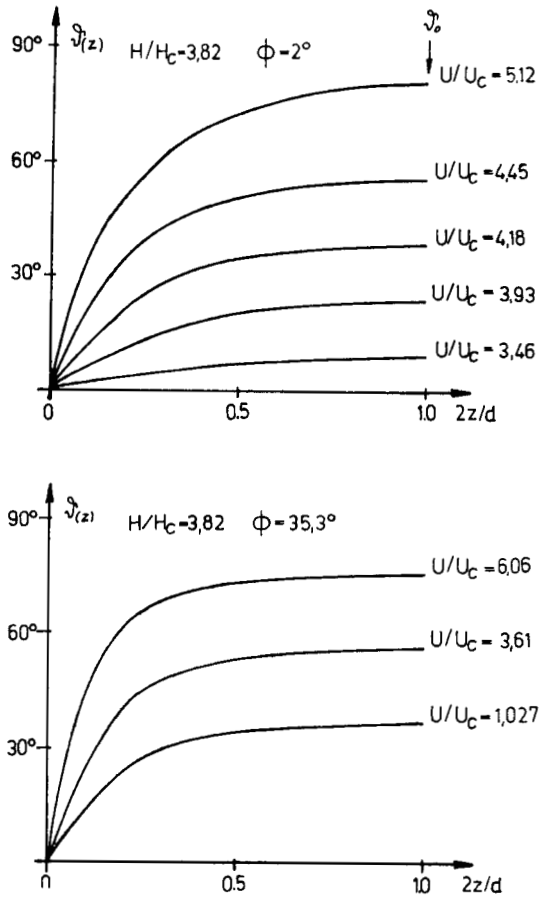

FIGURE 5 Calculated angle of deformation $\vartheta(z)$ *versus* coordinate z of the cell for $\Phi = 2°$ and 35.3°. ($\zeta = 1$ and $\eta = 0.5$).

Furthermore, the weak anchoring case can be obtained by a scaling procedure in the z-coordinate and fixing the z-origin at the point z_0 where $\vartheta(z_0) = \vartheta_{\text{surface}}$ which depends upon the surface energy.[4]

2.2. Proton-NMR line shape

Proton NMR absorption at a frequency ν in nematic and LC-phases is determined by the intramolecular dipolar Hamiltonian $\mathscr{H}_D$ which can be written in the form[5]

$$\mathscr{H}_D = S_\psi S \mathscr{H}_D^0 \tag{2.17}$$

where S is the molecular orientational order parameter, $\mathscr{H}_D^0$ is the

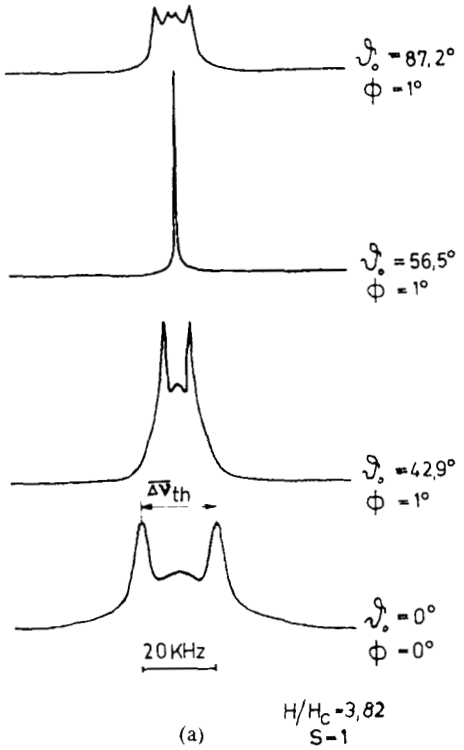

FIGURE 6 Theoretical (6a) and experimental (6b) proton-NMR line shapes for a nematic LC-sandwich cell (NPOB). The orientational order parameter S can be obtained by $S = \overline{\Delta\nu}\ \exp(U/U_c = 0,\ \Phi = 0°)/\overline{\Delta\nu}\ \text{theor}(\vartheta_0 = 0,\ \Phi = 0°)$. The calculation of the NMR-line shape has been performed using the experimental values of H/H_c, U/U_c, $\zeta = 1$ and $\eta = 0.5$.

The narrow central peaks in the experimental spectra are caused by a statistically oriented region in the sample (see section 4.1).

intramolecular dipolar spin hamiltonian for $S = 1$, and S_ψ depends upon the angle ψ between the director **n** and the external magnetic field **H**,

$$S_\psi = \tfrac{3}{2}\cos^2\psi - \tfrac{1}{2} \tag{2.18}$$

As a consequence of Eq. (2.17), the NMR-line shape $f_\psi(\nu)$ of a LC sample, with the director inclined at an angle ψ with respect to the magnetic field, is obtained from the line shape $f_0(\nu)$ of a LC sample, with its director along **H**, simply by a scaling procedure[5]

$$f_\psi(\nu) = \frac{1}{S_\psi} f_0\left(\frac{\nu}{S_\psi}\right) \tag{2.19}$$

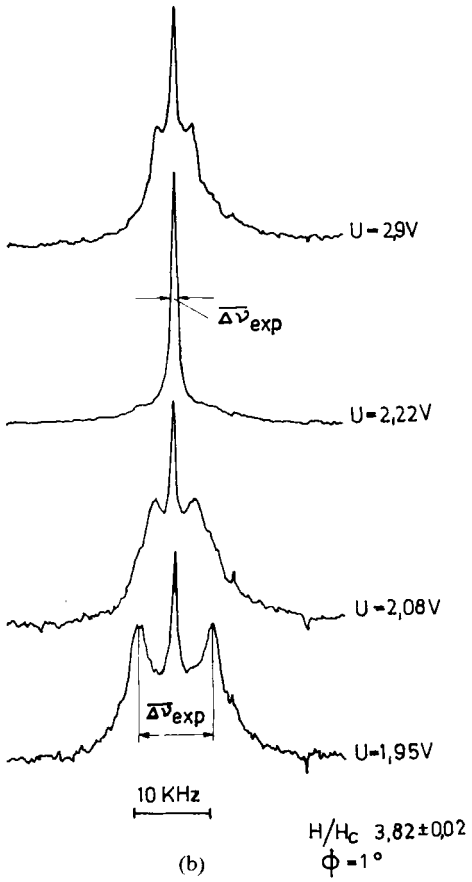

FIGURE 6 (*Continued*)

In the case of the deformed LC-layer (c.f. Figure 1), the angle $\psi = \Phi - \vartheta$ depends upon the coordinate z, and the NMR-line shape is a weighted superposition

$$\overline{f(\nu)} = \int_0^{\vartheta_0} f_{\phi-\vartheta}(\nu) w(\vartheta)\, d\vartheta \tag{2.20}$$

where $w(\vartheta)$ is the probability density function of the angle ϑ.

Thus, the analysis of the proton NMR-line shape of a LC-sample gives information about the orientational distribution $w(\vartheta)$ of the director in a LC-cell.

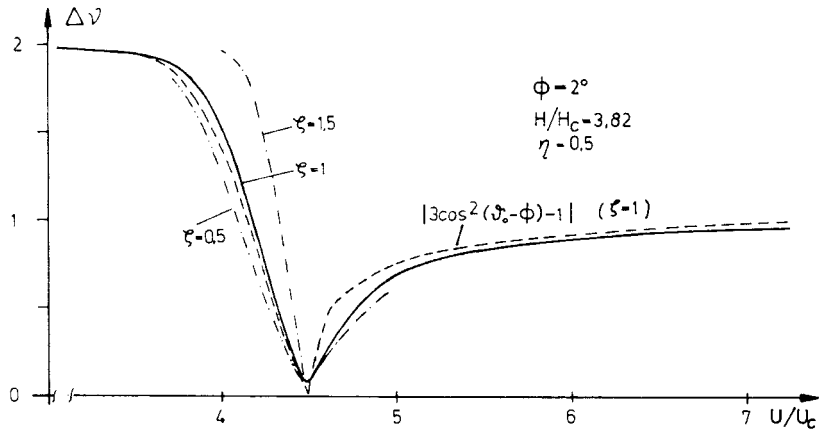

FIGURE 7 Relative splitting $\Delta\nu$ versus U/U_c for various values of dielectric anisotropy ζ. $\Delta\nu$ is defined as the ratio of the splitting $\overline{\Delta\nu}$ actually observed to the splitting $\overline{\Delta\nu}$ ($\psi = 90°$) which would be measured for an undeformed LC-sample where the director is exactly perpendicular to the magnetic field.

As an example, in Figure 6 the theoretical PMR-line shape $f_0(\nu)$ of NPOB well aligned along the magnetic field is given, together with some spectral patterns $\overline{f(\nu)}$ for deformed nematic layers.

The theoretical spectrum $\vartheta = 0°$ and $\phi = 0°$ was obtained from the molecular structure using the perturbation method described in ref. 5. $\overline{f(\nu)}$ has been calculated according to Eq. (2.20) using the scaling procedure (2.19) of $f_0(\nu)$ in Figure 6. The distribution function $w(\vartheta)$ was obtained by the method described in the previous section. It can be seen that the splitting $\overline{\Delta\nu}$ or the half width of the NMR-line is strongly affected by the values U/U_c, H/H_c, and Φ. In Figures 7 and 8, the theoretical dependence of the relative splitting $\Delta\nu = \overline{\Delta\nu}/(\overline{\Delta\nu}(\psi \equiv 90°))$ on U/U_c is shown for $H/H_c = 3.82$ and various directions ϕ of the magnetic field. If the LC-sample were uniformly aligned at the angle ϑ_0, the relative width should be

$$\Delta\nu = |3\cos^2(\vartheta_0 - \phi) - 1| \tag{2.21}$$

From Figure 7, in the case $\phi = 2°$, the influence of the nonuniform orientation of the director in the nematic cell forces the difference in line width to reach about 15%, which should be measured experimentally. The slope of $\Delta\nu$ is rather strongly dependent on the dielectric anisotropy $\epsilon_\parallel - \epsilon_\perp$ as can be seen from Figure 7 in the region of U/U_c giving the minimum line width $\Delta\nu$.

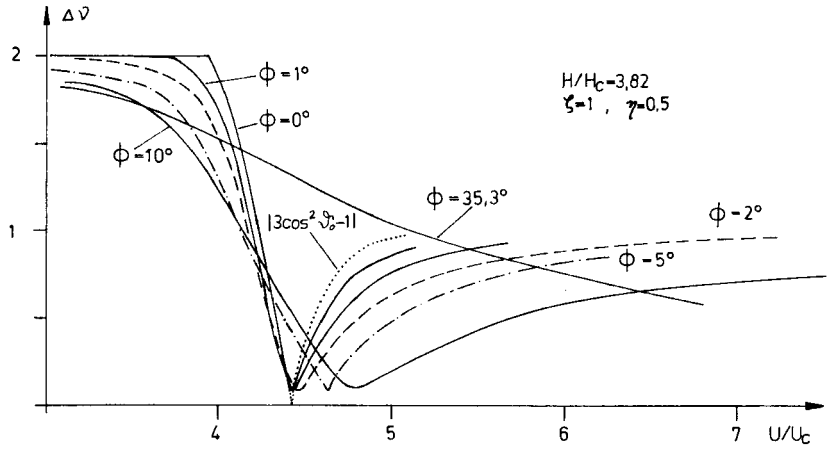

FIGURE 8 Normalized splitting $\Delta\nu$ *versus* U/U_c for various directions Φ of the magnetic field.

3. EXPERIMENTAL

Proton measurements have been performed using the Bruker NMR pulse spectrometer B-KR 322 s at resonance frequencies of 16, 32 and 60 MHz. To improve the S/N-ratio, in the case of LC-sandwich samples of 4...30 μm thickness (i.e. 0,75...6 mg of liquid crystal),

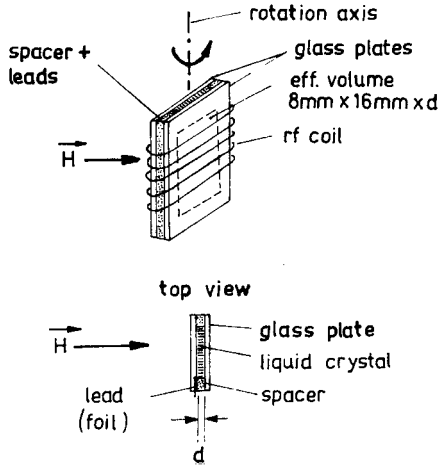

FIGURE 9 Principle construction of the NMR-cell. The size of the glass plates is 12 mm × 24 mm × 1.2 mm.

rectangular rf-coils have been used which gave a filling factor of about 10^{-3} to $8 \cdot 10^{-3}$. Figure 9 shows the main construction.

Accumulation of the FID signal with a number of sweeps between 1000 and 4000 followed by a Fourier transformation yielded S/N-ratios of about 10.

The proton-NMR signal of the empty cell (caused by protons in the spacers, glass plates etc.) had to be subtracted from the signal from the cell filled with the liquid crystal, in order to obtain the pure NMR-absorption signal of the nematic.

We used glass substrates with a conducting layer (*ca.* 100 Ω/cm^2) and, for planar alignment of the liquid crystal, a second layer of obliquely (60°) evaporated SiO[6].

The quality of the parallel orientation of the liquid crystal has been proved by microscopic observation with polarized light and measurements of capacitance in a magnetic field.

In most experiments with electric fields, we used sinusoidal voltage (0 – 8V) of 340 Hz.

The sample in the temperature-stabilized probe-head could be rotated about an axis perpendicular to the magnetic field. The liquid crystal material used in our experiments was 4-nitrophenyl 4-octyloxybenzoate (NPOB) the liquid crystalline properties of which are well known[7].

4. RESULTS AND DISCUSSION

4.1. NMR-samples without electric fields

To study the orientational distribution of the director, we have used LC-sandwich cells with thicknesses d of about 4 μm, 7 μm, 20 μm and 30 μm. The glass-surfaces had been treated to yield planar orientation of the director near the glass plates.

In Figure 10*a*, *b*, one can see the proton-NMR spectra at 32 MHz of a smectic–A NPOB-cell with $d = 20$ μm for $\phi = 0°$ and 90°. The sample had been cooled from the isotropic state ($T > 69\,°C$) to the smectic–A phase ($T = 59\,°C$) without a magnetic field. The central peak in both spectra comes from a region in the LC-cell where the director is randomly oriented. The relative size of the region (which is in Figure 10*a*, *b* about 30%) can be reduced if the sample is cooled from the isotropic phase to the S_A–phase in an orienting external magnetic field ($\phi = 0°$). As can be seen from Figure 10*c*, *d*, the central peak is much smaller, but still present (c.f. Figure 6b).

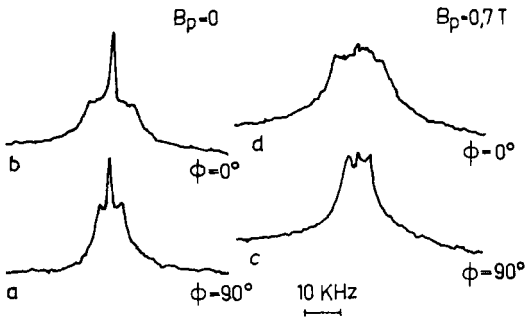

FIGURE 10 Proton NMR spectra of a NPOB-cell with $d = 20\ \mu$m in the smectic A phase. B_p is the value of the polarizing magnetic field (see text). $\nu_0 = 32$ MHz and $T = 59°C$.

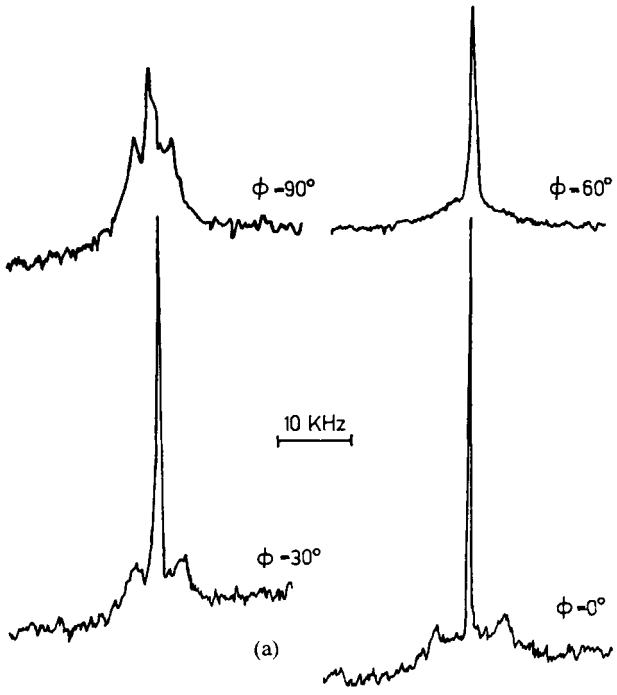

FIGURE 11 Experimental (11a) and theoretical (11b) angular dependence of PMR-line shape of a 4 μm-NPOB-cell at 32 MHz. Number of sweeps 4096, $T = 63.5°C$. Central peak see text).

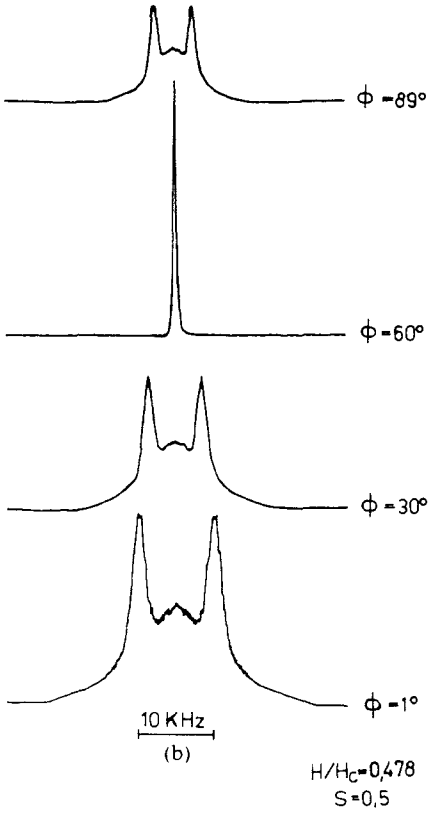

FIGURE 11 (*Continued*)

The dependence of the experimental PMR-line shape at 32 MHz on direction Φ of the magnetic field is shown in Figure 11 for the 4 μm-cell. The changes in the line shape are caused by deformations of the director field. Theoretical line shapes have been calculated according to Eq. (2.20) using values $H/H_c = 0.478$, $\eta = 0.5$. In Figure 12, the dependence of the relative splitting $\Delta\nu$ and the maximum deformation angle ϑ_0 upon the direction Φ of the magnetic field is shown for the same sample.

It can be seen that the normalized experimental splitting $\Delta\nu$ differs very little from the dependence $\Delta\nu = (\frac{3}{2}\cos^2\phi - \frac{1}{2})$, because in this case $H/H_c = 0.48$ and ϑ_0 remains small. For higher values of cell thickness d at the same resonance frequency $\nu_0 = 32$ MHz, the LC-layer becomes more deformed and the angular dependence of $\Delta\nu$ is strongly changed.

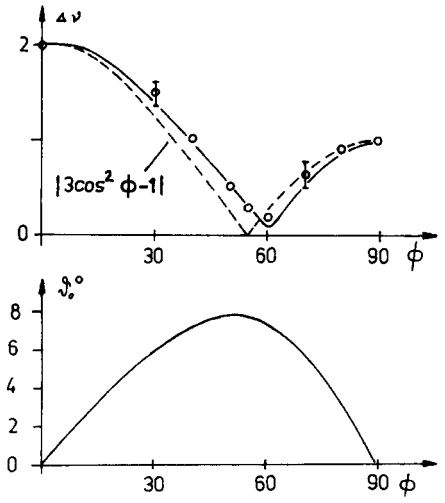

FIGURE 12 Relative splitting $\Delta\nu$ and ϑ_0 *versus* Φ for the 4μm-NPOB-cell at $T = 63.5\,^{\circ}$C and $\nu_0 = 32$ MHz. Circles correspond to experimental values; the solid line is the theoretical dependence for $H/H_c = 0.478$ and $\eta = 0.5$).

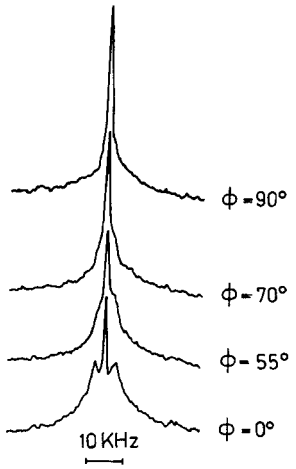

FIGURE 13 Angular dependence of the PMR-line shape of NPOB at 32 MHz for a cell of 7 μm thickness at $T = 67\,^{\circ}$C.

Figure 13 shows the angular dependence of the proton NMR-line shape at 32 MHz for $d = 7\ \mu$m and NPOB in the nematic phase ($T = 67\,^{\circ}$C). The spectrum at $\Phi = 0^{\circ}$ can be interpreted as the signal of a sample with 75% parallel-oriented LC, the remaining 25% being randomly distributed. Parts with random orientation are caused most probably by some surface alignment effects near the edges of our NMR samples and partially by faulty surface treatment.

4.2. NMR samples with electric fields

In Figures 14 and 15, the PMR-line width $\Delta\nu$ is plotted as a function of the voltage U/U_c at the LC-cell for $\nu_0 = 16$ and 32 MHz, where the direction of the magnetic field has been chosen to be 1°, 5°, 10°, and 35°. The LC-sample thickness is $d = (30 \pm 1)\ \mu$m. Similar results have been obtained for $\nu_0 = 60$ MHz. It can be seen that there is a small but distinct difference between the experimental values of $\Delta\nu$ and the simplified dependence given by Eq. (2.21), whereas the experimental points are adequately described by means of the theory developed in section 2.

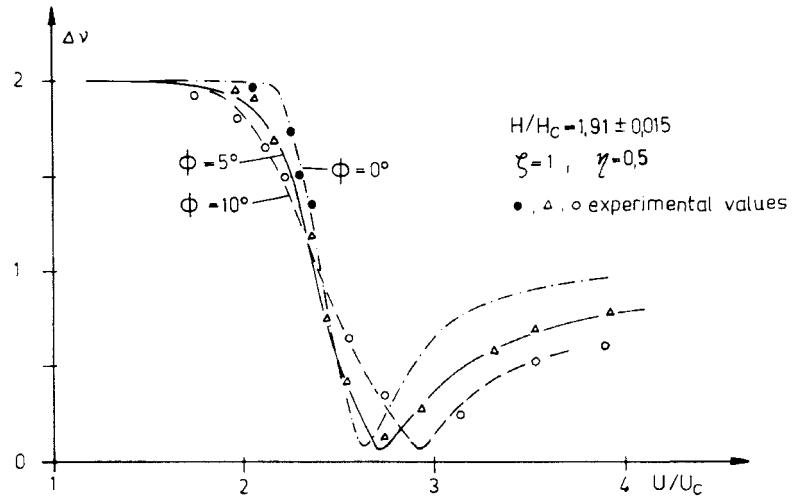

FIGURE 14 Experimental values of relative splitting $\Delta\nu$ *versus* U/U_c for a NPOB-cell of 30 μm thickness at $T = 63.5\,^{\circ}$C and $\nu_0 = 16$ MHz. Theoretical fit with $\zeta = 1$ and $\eta = 0.5$.

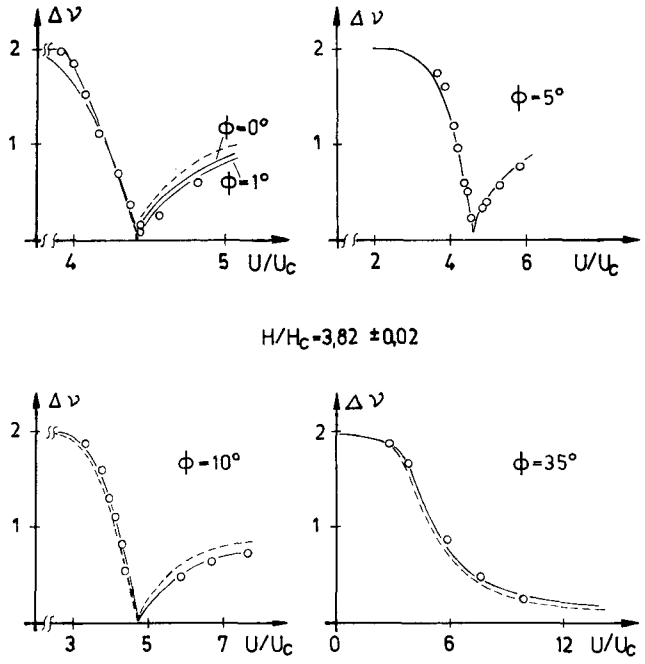

FIGURE 15 The same as in Figure 14 except $\nu_0 = 32$ MHz ($H/H_c = 3.82$). The dotted lines correspond to the simplified dependence (2.21). Experimental values (circles) are adequately described by the theory developed in section 2 (solid lines). Similar results have been obtained for $d = 9$ μm and 19 μm.

4.3. Conclusion

As was pointed out in section 2.2, the proton NMR-line shape $\overline{f(\nu)}$ of a LC-sample (consisting of regions with different orientations of the nematic director) contains information about the relative size $w(\psi)$ of the regions where the director forms the angle ψ with the direction of the external magnetic field. Therefore, by means of NMR-line shape analysis it should be possible to obtain the distribution function $w(\psi)$ of the director in the sample. Whereas the measurement of the capacitance C or the optical phase-difference angle δ[2] in LC-samples gives as a result a number (C or δ) depending in an integral manner on the distribution function of the director, the result of the NMR-measurement is the function $\overline{f(\nu)}$, i.e., a whole set of integrals $\overline{f(\nu_i)}$ (Eq. 2.20). We have seen that the experimental proton NMR-line shape of nematic sandwich cells could be simulated using the theory

described in section 2. Thus, by means of a fitting procedure, various parameters of the liquid crystal such as elastic constants (K_1, K_3) and/or dielectric or diamagnetic permittivities, can be obtained from NMR-line shape analysis.

Acknowledgments

The authors are grateful to Dr. Grande for fruitful discussions. Furthermore, we wish to thank Dr. Koswig and Dr. Hauck (ZIE AW DDR Berlin) and Dipl.-Phys. F. Jilek (KMU Leipzig) for their help in evaporation techniques.

References

1. A. Saupe, *Z. Naturforsch.*, **15a**, 815 (1960).
2. H. Gruler, T. J. Scheffer and G. Meier, *Z. Naturforsch.*, **27a**, 966 (1972).
3. H. J. Deuling, *Mol. Cryst. Liq. Cryst.*, **19**, 123 (1972).
4. P. G. De Gennes, "*The Physics of Liquid Crystals*", Oxford, Clarendon Press, 1974.
5. H. Schmiedel, B. Hillner, S. Grande, A. Lösche and S. Limmer, *J. Magn. Res.*, **40**, 369 (1980).
6. L. A. Goodman, *RCA Rev.*, **35**, 447 (1974).
7. D. Demus, Forschung über flüssige Kristalle, Martin-Luther-Universität Halle-Wittenberg, *Wiss. Beitr.*, **21** (1978) N7.